WCTE
WORLD CONFERENCE ON TIMBER ENGINEERING
2010

ENHANCED PERFORMANCE OF LONGITUDINALLY POST-TENSIONED LONG-SPAN LVL BEAMS

Alessandro Palermo[1], Stefano Pampanin[2], David Carradine[3], Andrew H. Buchanan[4], Bruno Dal Lago[5], Claudio Dibenedetto[5], Simona Giorgini[5], Paola Ronca[6]

ABSTRACT: The scope of this paper is to highlight the advantages of using longitudinally post-tensioning for long-span timber beams compared to traditional glulam or LVL solutions. The analysis is limited to serviceability limit states for gravity loads. An analtycal iterative procedure which takes into account tendon elongation within beam deflecting has been implemented and validated through experimental tests carried out at the University of Canterbury.In particular, two different static configurations have been studied and different tendon profile configurations (straight and draped) internal and external to the beam section have been investigated and compared with traditional solid timber beams.
The experimental results confirm the enhanced performance in terms of deflections at serviceability limit state of the longitudinally post-tensioned solutions with respect to traditional timber beams, especially if external draped tendons are adopted.

KEYWORDS: Longitudinally post-tensioned timber, Long-span LVL beams, Unbonded post-tensioning

1 INTRODUCTION

Post-tensioning was started by Fressynet (1928) with concrete members with the intent to improve the overall structural performance under external loads when long span beams and / or bridges are targeted.
The same technology relying on unbonded post-tensioned tendons / bars can be easily applied to timber.
Deflection limit states typically govern design of timber members which are typically characterised by high flexibility due to low values of both elastic and shear moduli.
The introduction of post-tensioning allows an apparent reduction in the effects of external loads. In fact, post-tensioned tendons can be designed to balance external loads, typically dead loads plus part of live loads. This obviously allows designers to reduce member depth without affecting the overall flexibility of the structure. However these benefits of post-tensioning could be drastically reduced by long-term effects, such as creep and shrinkage. However, recent studies [1][2] confirmed that post-tensioning losses can be estimated around 25% in the worst environmental scenario.
Despites long-term effect issues, this technology has already easily met typical requirements of exhibition, industrial and commercial buildings as confirmed by the recent commercial constructions in New Zealand [3].
In this paper, the investigation is limited to instantaneous behaviour of longitudinally post-tensioned timber LVL (Laminated Veneer Lumber) beams using several tendon profiles.
This research work explores LVL only, as an engineered timber, but similar outcomes can be achieved if glulam (glue laminated timber) is adopted.
Since the compressive strength is considerably higher than the tensile strength for these engineered wood products, the application of post-tensioning becomes more efficient since compression failure of top timber fibers is expected.
Several tendon profiles are herein investigated and compared considering two static schemes. Both numerical and experimental investigations are presented.
Finally a parametric analysis is carried out with the aim to define load span tables which easily allow the preliminary design to quantify the reduction in beam depth for different tendons profiles, compared to traditional solutions.

[1] Senior Lecturer, Department of Civil and Natural Resources Engineering, University of Canterbury, New Zealand. Email: alessandro.palermo@canterbury.ac.nz
[2] Associate Professor, Department of Civil and Natural Resources, University of Canterbury, New Zealand. Email: stefano.pampanin@canterbury.ac.nz
[3] Timber Research Engineer, Department of Civil and Natural Resources Engineering, University of Canterbury, New Zealand. Email: david.carradine@canterbury.ac.nz
[4] Full Professor, Department of Civil and Natural Resources Engineering, University of Canterbury, New Zealand. Email: andy.buchanan@canterbury.ac.nz
[5] Research Engineers, Department of Structural Engineering, Politecnico di Milano, Italy.
[6] Full Professor, Department of Structural Engineering, Politecnico di Milano, Italy. Email: ronca@stru.polimi.it

2 USE OF POST-TENSIONING FOR TIMBER STRUCTURES

Two types of post-tensioning have been adopted for timber, transversal post-tensioning which is typically applied perpendicular to the timber grain and longitudinal post-tensioning, i.e. parallel to timber fibres.

2.1 TRANSVERSAL POST-TENSIONING

Transversal post-tensioning started within applications to bridge decks; this technology was born in Canada (1976) [4][6] as an alternative to nail laminated wood decks which were considerably deteriorating during their bridge lifetimes. The technology is based on the use of high strength unbonded post-tensioning bars and steel anchorage plates which transversely clamp sawn timber deck boards from one side to the other.

Different deck systems were developed such as parallel chord, "T" and "box" beam decks, and cellular deck systems. Vierendeel truss deck systems guaranteed good structural performances and easy fabrication (
Figure **1**a).

In the stress laminated timber "T" beam decks the shear connection between beams and deck is given by post-tensioning only without mechanical fasteners (
Figure **1**b).

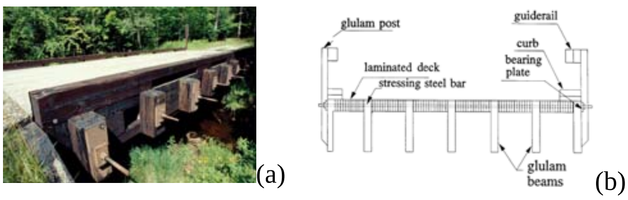

Figure 1: *Transversal post-tensioning: (a) Experimental Vierendeel truss deck at Mormon Creek, North Michigan (b) Schematic view of the T-beam stress laminated timber deck [7]*

An alternative solution to a "T" section beam deck is multiple box girders that provides an excellent structural option if spans in the range of 9 to 24 meters are targeted (Figure 2).

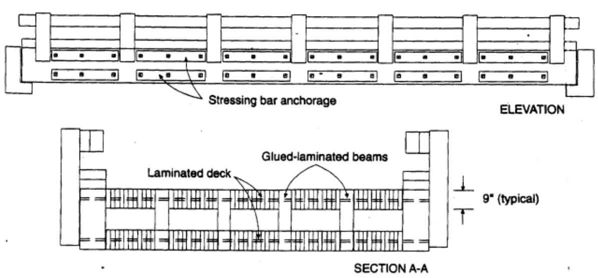

Figure 2: *Typical details for stress laminated timber box beam bridge decks [7]*

Cellular stress laminated timber deck systems use thinner, closer spaced webs with two transversely laminated flanges. Despite the high speed of construction and low cost of this technology, several issues such as long-term post-tensioning perpendicular to the grain and durability are still under investigation.

2.2 POST-TENSIONED TIMBER BUILDINGS

In the last two decades innovative seismic structural systems for buildings based on longitudinal post-tensioning have been investigated for concrete and recently extended to timber. The development of damage control design philosophies lead to innovative seismic resistant systems, named jointed ductile connections that allow discrete dissipative mechanisms placed in specific locations in the structure; they were previously developed for precast concrete structures (Priestley, 1991 [8], 1996 [9], Priestley et al., 1999 [10], Pampanin, 2005 [11]), and successfully transferred to timber frames (Palermo et al., 2005 [12], 2006 a, b [13] and walls (Smith et al., 2007 [14]), Figure 3. This Pres-Lam® concept extended to timber members represents a viable option for multi-storey timber buildings and is protected by an international patent [15]. This system was firstly tested for the beam-to-column subassembly, then wall-to-foundation and column-to-foundation connections, as shown in Figure 4.

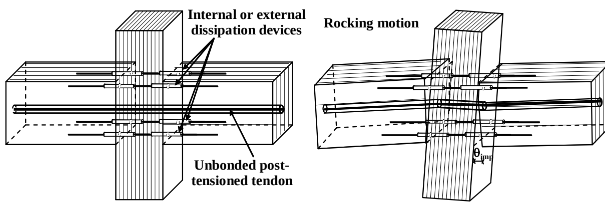

Figure 3: *Basic concept of hybrid jointed ductile connections for LVL frame systems [13]*

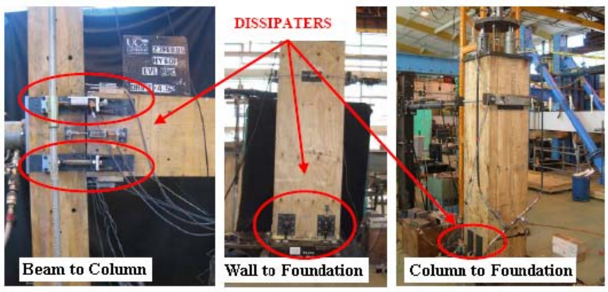

Figure 4: *Tests carried out at the University of Canterbury on hybrid system for timber structures [16]*

Given the advantages that this solution offers for seismic resistant timber frames it is natural to extend and investigate longitudinal post-tensioning for timber frames subjected to vertical loads. This investigation is limited to post-tensioned timber beams designed for gravity loads.

3 NON-LINEAR ANALYSIS FOR EXTERNAL UNBONDED POST-TENSIONED TENDONS

The analysis of post-tensioned timber beams can be complicated by geometric non-linearities. If the deformed configuration of a beam subjected to vertical loads is not negligible it can affect the internal tendon forces which are modified by the beam configuration causing an additional elongation. This elongation depends on beam deflection, and the stress variation in each tendon is member dependent since there is no bond between steel and timber.

Moreover, since the elastic modulus of timber is smaller than that of concrete, this contribution is amplified. This affects the final deformed configuration of the beam and hence the final tension force in the tendons. In addition, the shear contribution in timber is not negligible and this amplifies the above mentioned non-linear effects, starting from the serviceability limit state. Typically these tendon elongation rates are an additional positive contribution in terms of deformation but a clear check has to be done in order to avoid possible premature yielding of tendons.

Several authors have investigated unbonded post-tensioned concrete beams at the ultimate limit state, while a few published works have dealt with the analysis of unbonded prestressed concrete members in the elastic range, including Balanguru (1981) [17], Naaman (1987 [18], 1990 [19]). These works proposed a method to reduce the analysis of beams with unbonded tendons to that of beams prestressed with bonded tendons through the use of a strain reduction (or bond reduction) coefficient [20], which is defined differently for elastic uncracked states and elastic cracked states.

At this stage, an iterative procedure is herein applied for unbonded post-tensioned timber beams with the intent to successively propose specific strain coefficients considering different tendon profiles. Since the tendon elongation increases the stresses in the tendons, a new displacement $v(x)$ and rotations $\varphi(x)$ of beam's edges can be calculated considering the increment of tendon elongation ΔL_i. This procedure requires several iterative steps and is repeated several times until convergence is reached. Figure 5 briefly summarizes this concept.

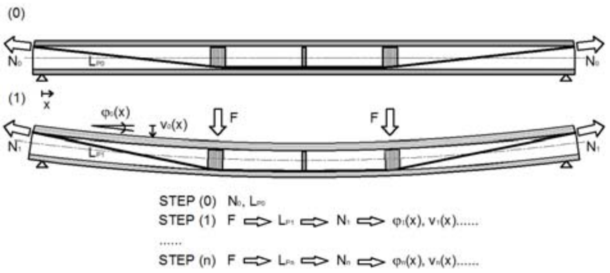

Figure 5: *Non-linear unbonded post-tensioned tendons concept*

At step (0) the initial load N_0 is applied; after the application of the forces F, step (1), the beam changes its configuration and the tendon length L_{P0} increases to reach a value L_{P1}; this tendon strain produces an increase of the post-tensioning load to N_1. Since the beam initial configuration depends on the pre-camber due to the post-tensioning only, if the post-tensioning load changes the deformed configuration changes too. Dividing the tendon profile into finite segments the length of the single elements $l_{P0,i}$ can be calculated with Pitagora's theorem (Eq. 1):

$$l_{P0,i} = \sqrt{\left(x_{P0,i} - x_{P0,i-1}\right)^2 + \left(y_{P0,i-1} - y_{P0,i}\right)^2} \qquad (1)$$

where x_{P0} and y_{P0} are the initial coordinates at the edges relative to the reference system. In this way the initial length of the cable L_{P0} can be achieved as sum of the length of the single elements (Eqs. 2-3):

$$L_{P0} = \sum_{i=1}^{n} l_{P0,i} \qquad (2)$$

$$L_{P0} = \sum_{i=1}^{n} \sqrt{\left(x_{P0,i} - x_{P0,i-1}\right)^2 + \left(y_{P0,i-1} - y_{P0,i}\right)^2} \qquad (3)$$

The length L_{P0} obtained in a continuous system is achieved using infinitesimal lengths dx and dy; this alternative expression is shown in the Eq. 4:

$$L_{P0} \cong \int_0^L \sqrt{dx_p^2 + dy_p^2} \qquad (4)$$

After the application of the load the tendons configuration depends on the elastic deformation of the beam. Eq. 5 represents the single element $l_{P1,i}$ while length of the tendon at step 1 L_{P1} is given by Eq.6:

$$l_{P1,i} = \sqrt{\left(x_{P1,i} - x_{P1,i-1}\right)^2 + \left(y_{P1,i-1} - y_{P1,i}\right)^2} \qquad (5)$$

$$L_{P1} = \sum_{i=1}^{n} l_{P1,i} \qquad (6)$$

The length variation of the tendon at step 1 ΔL_1 is reported in Eq. 7:

$$\Delta L_1 = L_{P1} - L_{P0} \qquad (7)$$

Starting from the tendon elongation the strain at step 1 ε_1 can be achieved as shown in Eq. 8:

$$\varepsilon_1 = \varepsilon_0 + \frac{\Delta L_1}{L_{P0}} \qquad (8)$$

where ε_0 is the initial deformation. Eq. 9 shows the new force in the tendon N_1^* since the deformation at step 1 ε_1 previously determined:

$$N_1^* = \varepsilon_1 \cdot A_P \cdot E_P \qquad (9)$$

where A_P is the post-tensioning area and E_P the steel elastic modulus. Eq. 10 reports the force variation of the tendon at step 1, ΔN_1^*:

$$\Delta N_1^* = N_1^* - N_0 \qquad (10)$$

where N_0 is the initial force. However this increase of force is subjected to instantaneous losses; the force in the tendon N_1* has to be depurated of the instantaneous elastic losses $\Delta N_{\Delta N1}^{(inst)}$. as reported in Eq. 11:

$$\Delta N_1^* - \Delta N_{\Delta N1}^{(inst)} = \Delta N_1 \qquad (11)$$

Finally, the tendon force at step 1 (Eq. 12) N_1 is:

$$N_1 = N_1^* - \Delta N_{\Delta N_1}^{(inst)} \qquad (12)$$

Knowing N_1 it is possible to determine a new slope and a new displacement profile of the beam, and repeat the

step-by-step procedure until convergence is reached ($N_n \cong N_{n-1}$), typically after five or six iterations.
The iterative procedure at step *n* is reported in the flow chart below (Figure 6).

$$\boxed{\Delta L_n = L_{Pn} - L_{Pn-1}} \Rightarrow \boxed{\varepsilon_n = \varepsilon_{n-1} + \frac{\Delta L_n}{L_{n-1}}} \Downarrow$$

$$\boxed{\Delta N_n = N_n^* - N_{n-1}} \Leftarrow \boxed{N_n^* = \varepsilon_n \cdot A_P \cdot E_P} \Leftarrow$$

$$\Rightarrow \boxed{N_n = N_n^* - \Delta N_{\Delta N_n}^{(inst)}}$$

Figure 6: *Iterative procedure at step n*

The recurrent formula is shown in Eq. 13:

$$N_n = A_P \cdot E_P \cdot \left(\varepsilon_{n-1} + \frac{\Delta L_n}{L_{n-1}} \right) - \Delta N_{\Delta N_n}^{(inst)} \qquad (13)$$

This iterative procedure has been implemented and verified within experimental tests quantifying the tendon elongation contribution.

4 EXPERIMENTAL PROGRAM

4.1 TESTING PROGRAM

Tests have been carried out on vertically loaded Laminated Veneer Lumber (LVL) beams with longitudinal unbonded post-tensioned tendons. These beams were designed as an LVL post-tensioned alternative solution for a feasibility study of a multi-storey building, the School of Biological Science at the University of Canterbury, now under construction with concrete technology.

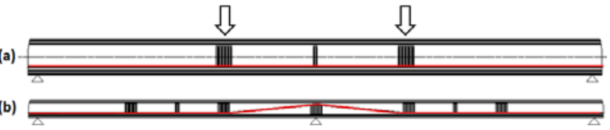

Figure 7: *Straight tendon profile configuration – (a) Simply supported beam (b) Statically indeterminate beam*

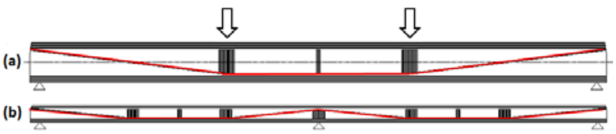

Figure 8: *Draped tendon profile configuration – (a) Simply supported beam (b) Statically indeterminate beam*

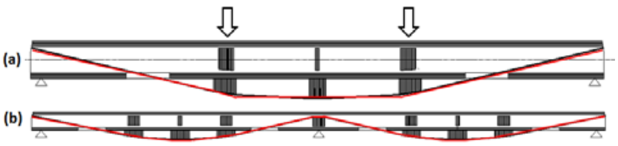

Figure 9: *High eccentricity tendon profile configuration – (a) Simply supported beam (b) Statically indeterminate beam*

Two different static schemes were considered, a simply supported beam and a statically indeterminate beam (three supports). The first was a full scale prototype while the second one is 1:2 scale. The different tendon profiles and load configurations are shown in Figures 7, 8 and 9.

For each static scheme, different tendon profiles were investigated in order to compare the benefits in terms of depth reduction for straight tendon (named bottom configuration), draped tendon (named top configuration), and external draped tendon (named external configuration). Moreover, a "benchmark" timber beam without post-tensioning was tested in order to emphasise the enhanced performance of post-tensioned beams.

In Table 1, for each beam type a summary of the testing program is reported, along with number of tendons and initial post-tensioning force applied. In Table 2 loading sequence is shown.

Table 1: *Testing program*

	Test code	Description	Test scale	No. Tendons	Initial Post-tensioning force [kN]
Simply supported beam	1 Benchmark	Without post-tensioning	1:1	none	none
	1 Bottom	With post-tensioning on the bottom of the beam end	1:1	6	130
	1 Top	With post-tensioning on the bottom of the beam end	1:1	6	130
	1 External	With external draped tendons due to external deviators	1:1	2	130
Statically indeterminate beam	2 Benchmark	Without post-tensioning	1:2	none	none
	2 Bottom	With post-tensioning on the bottom of the beam end	1:2	3	130
	2 Top	With post-tensioning on the bottom of the beam end	1:2	3	130
	2 External	With external draped tendons due to external deviators	1:2	1	120

Table 2: *Load sequence*

Final sequence	Correspondent load	
Load [kN]	Heavy floor package	Light floor package
0	Precamber	
50		Dead
90	Dead	30% Live
140	30% Live	70% Live
190	70% Live	SLS
230	SLS	
250	Load cell capacity limit	

The load sequence was calibrated in order to represent two types of floors; respectively a heavy (1.838 kN/m^2) and light (0.933 kN/m^2) package.

4.2 SECTIONS

Rectangular hollow core section has been adopted for both beam types. Figure 10 shows the LVL section profiles for the simply supported beam and the statically indeterminate beam. Figure 11 shows a simply supported beam under construction while Figure 12 gives a detail view of an internal deviator. Figure 13 and Figure 14 show the details of external deviators, for two different static schemes.

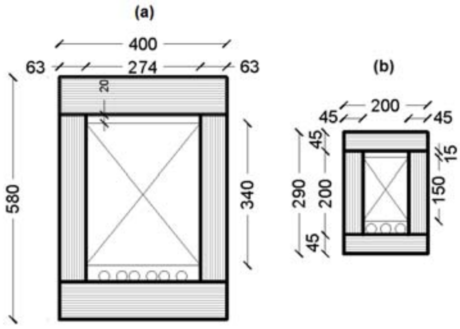

Figure 10: *LVL sections – (a) Simply supported beam (b) Statically indeterminate beam*

Figure 11: *Beam construction*

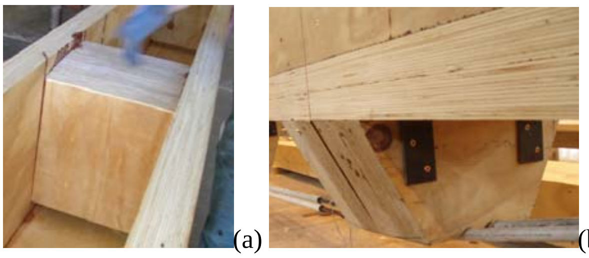

(a) (b)

Figure 12: *Beam detail view (a) internal deviator (b) external deviators*

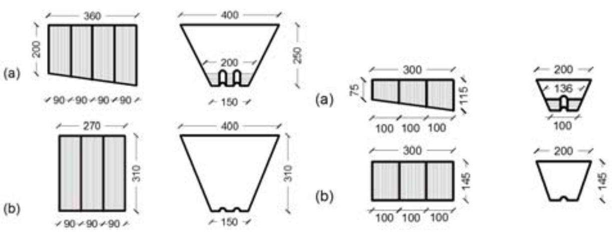

Figure 13: *Beam 1 - External deviators (a) Lateral (b) Central -* ***Figure 14:*** *Beam 2 - External deviators (a) Lateral (b) Central*

4.3 MATERIALS

Table 3 and Table 4 show timber and post-tensioning steel characteristics.

Table 3: *LVL mechanical characteristics*

f_b [MPa]	f_c [MPa]	f_t [MPa]	f_s[MPa]	f_p[MPa]	E [MPa]	G [MPa]
48	45	30	6	12	10700	535

Where f_b is the bending strength, f_c is the compression strength, f_t is the tension strength, f_s is the shear in beams, f_p is the compression perpendicular to grain strength, *E* is the modulus of elasticity, *G* is the modulus of rigidity. Both elastic and rigidity modulus are parallel to the fibres. It is important to highlight that for timber, since the Poisson's coefficient is very high, the shear contribution (tangential elastic modulus G) increments the flexural deformation in a range which varies from 5% to 20%.
In the numerical predictions, shear effect has been considered referring to Timoshenko's beam theory [21].

Table 4: *Post-tensioning steel characteristics*

f_{ptk} [MPa]	f_{ptk1} [MPa]	E [MPa]	A [mm^2]
1860	1674	195000	100,1 (7 wires strands)

Where f_{ptk} is the ultimate tensile stress, f_{ptk1} is the characteristic strength at 0,1% of deformation ($0.9\ f_{ptk}$), *E* is the modulus of elasticity.

4.4 TEST SETUP

A steel reaction frame firmly linked to the strong floor hosted the central ram. The load was applied through a reinforced steel beam in two points (l/3 and 2/3 of the total support span). A similar setup was used for the statically indeterminate beam, where the load was applied at the middle of each span (l/4 and 3/4).
Displacements, load and post-tensioning forces, and strains have been recorded. For measurement, rotary potentiometers and straight 50 mm potentiometers have been used. For each tendon load cells were used to monitor post-tensioning forces. Deformations have been measured by strain gauges.

4.4.1 Simply supported beam

Figure 15 and Figure 16 show the test setup for the simply supported beam.

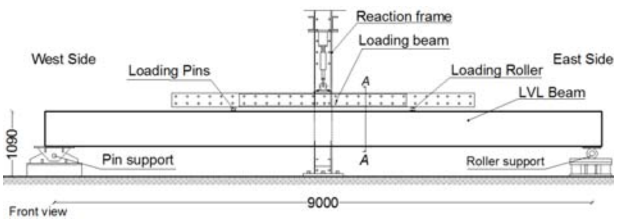

Figure 15: *Test setup simply supported beam - Front view*

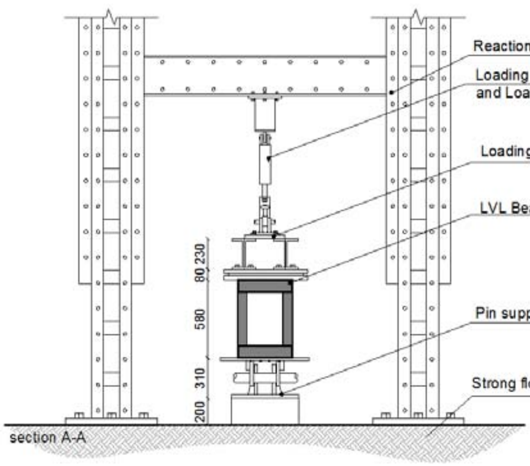

Figure 16: *Test setup simply supported beam - Section A-A*

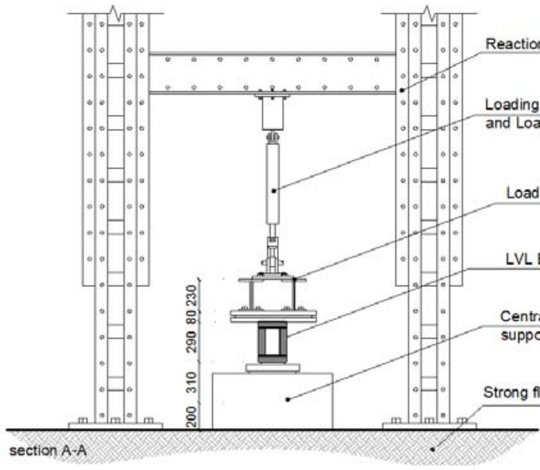

Figure 20: *Test setup statically indeterminate beam - Section A-A*

Figure 17 and 18 show examples of acquisition scheme for experimental data. Deflections were recorded by 4 rotary potentiometers (two for each side of the central section, one at l/3 and one at 2/3) and two straight potentiometers (one at l/6 and one at 5/6). Forces were recorded by the central ram load cell and one load cell for each tendon.

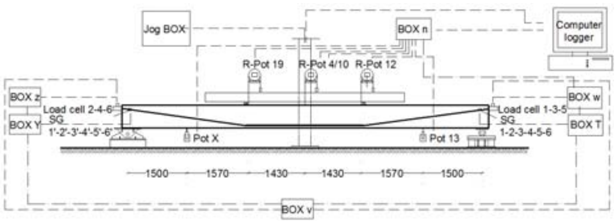

Figure 17: *Acquisition scheme – Simply supported beam and draped tendons*

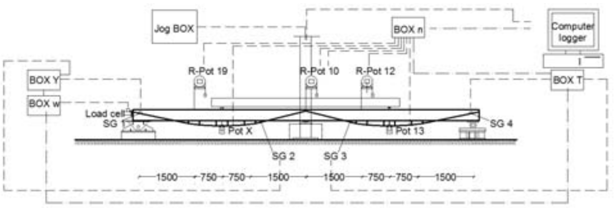

Figure 18: *Acquisition scheme – Statically indeterminate beam and external tendons*

4.4.2 Statically indeterminate beam

Figure 19 Figure 20 show the test setup for the statically indeterminate beam; The actuator is kept in the same position hence one concentrated load per span is applied to the beam.

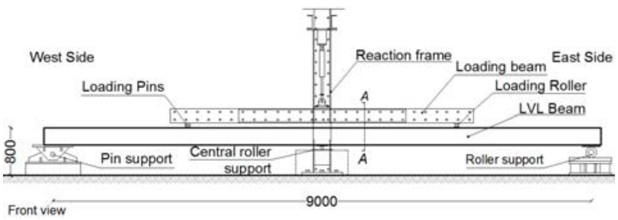

Figure 19: *Test setup statically indeterminate beam - Front view*

Details for transferring post-tensioning force is shown in Figure 21. Steel plates with longitudinal stiffeners are introduced in order to properly spread the load to the timber fibres. Similar details have been adopted for different tendon profiles, as shown in Figure 22 for respectively Bottom, Top and External configuration.

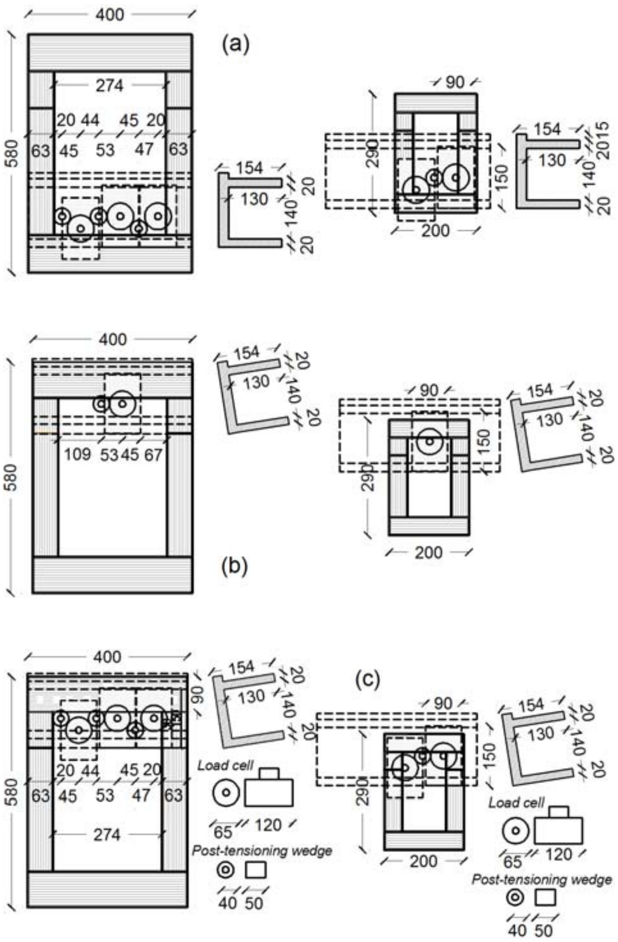

Figure 21: *Anchorage plates test setup – (a) Bottom configuration (b) Top configuration (c) External configuration*

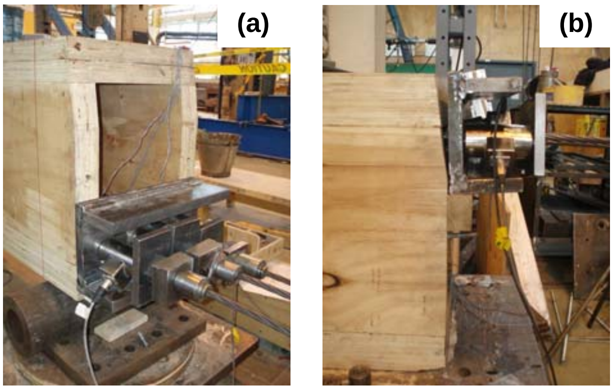

Figure 22: *Plates detail – (a) Bottom configuration (b) Top configuration for simply supported beam*

5 TEST RESULTS

Tests on benchmark timber beams have also been used to obtain the real elastic modulus of timber. For sake of brevity, only maximum displacements are respectively herein reported in Tables 5, 6. The stiffening effect has been confirmed by the tests as previously introduced in paragraph 3 (Figure 5 and Figure 6). The iterative procedure previously presented has been implemented and satisfactory results were obtained in most cases. Figure 23, 24, 25 – Figure 27, 28, 29 show the displacement along beam axis for different load conditions comparing numerical and experimental results.

5.1 SIMPLY SUPPORTED BEAM

It can be observed that an overall satisfactory prediction of the iterative procedure for most load levels with the experimental results was obtained (Table 5). For between beams with Bottom (Figure 23) and Top configuration (Figure 24) there is a good correspondence in terms of displacement performance.

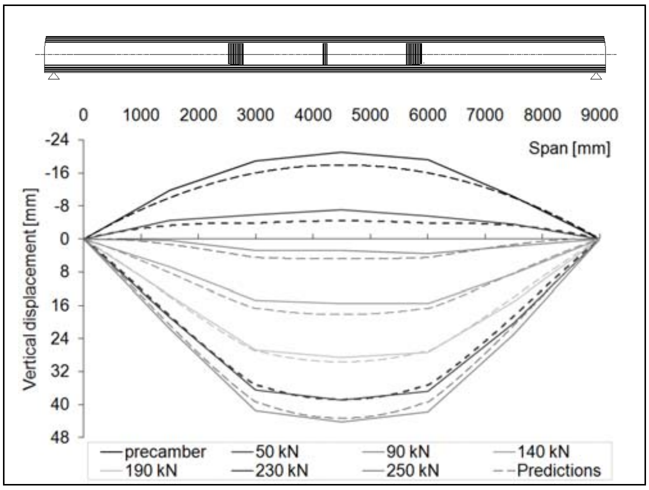

Figure 23: *Beam 1 - Comparison of numerical and experimental displacements: straight profile (Bottom)*

The solution with external tendons (External) works very similarly since it has been designed to achieve similar displacements but less tendons are adopted with respect to the other two solutions (two instead of six).

Table 5 summarises results in terms of displacements shown in Figures 23-25. Looking at the load level corresponding to 130 kN (very close to SLS for light floor package) it is clear how the introduction of post-tensioning provides a reduction of 60% of maximum displacement of the beam.

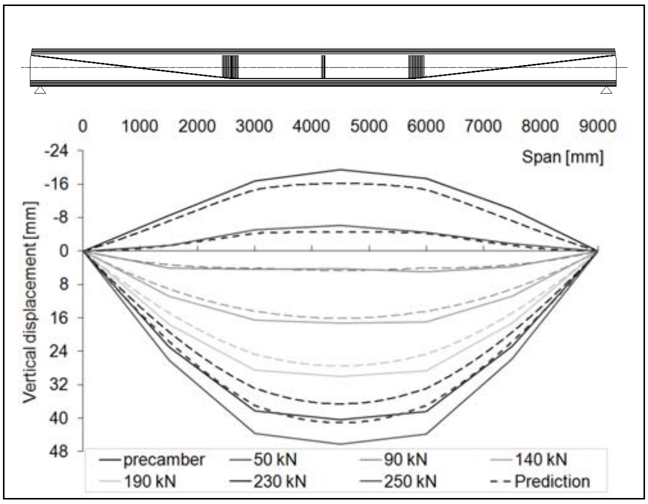

Figure 24: *Beam 1 - Comparison of numerical and experimental displacements: draped profile (Top)*

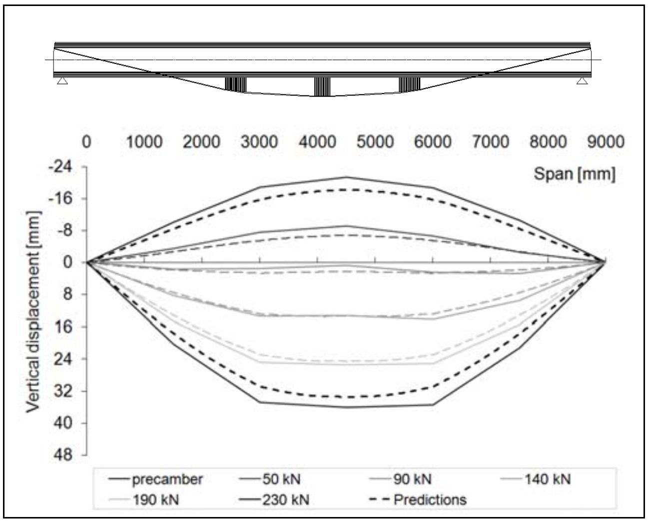

Figure 25: *Beam 1 - Comparison of numerical and experimental displacements: External profile*

Table 5: *Beam 1: Maximum deflections experimental (white column) and numerical (grey column)*

	Displacement (mm)							
Load [kN]	Benchmark		Bottom		Top		External	
0	0,00	0,00	-20,94	-17,92	-19,37	-16,20	-21,39	-18,14
50	13,68	14,56	-8,13	-4,38	-6,19	-4,60	-9,18	-6,80
90	24,57	25,13	2,85	4,83	4,45	4,63	0,64	2,22
130	35,21	-	12,72	-	13,41	-	11,21	-
140	-	-	15,52	18,18	17,26	16,10	13,22	13,43
190	-	-	28,56	29,64	30,31	27,50	25,44	24,57
230	-	-	38,85	38,75	40,95	36,56	36,09	33,43
250	-	-	44,26	43,29	46,19	41,07	-	-

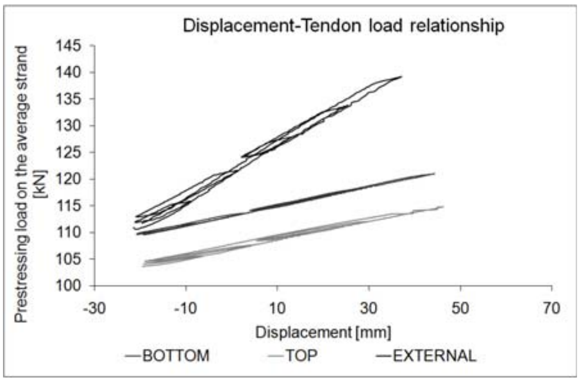

Figure 26: *Beam 1 – Displacement / tendon load relationship*

Figure 26 shows that the increase of force in the tendons while loading the beams can be quantified as a small percentage in the cases of internal configurations (5-8%), while higher values (25%) can be observed for the external tendon profile.

5.2 STATICALLY INDETERMINATE BEAM

Similar considerations can also be stated for statically indeterminate beam prototypes. Only some discrepancies have been found for the correct prediction of the precamber.

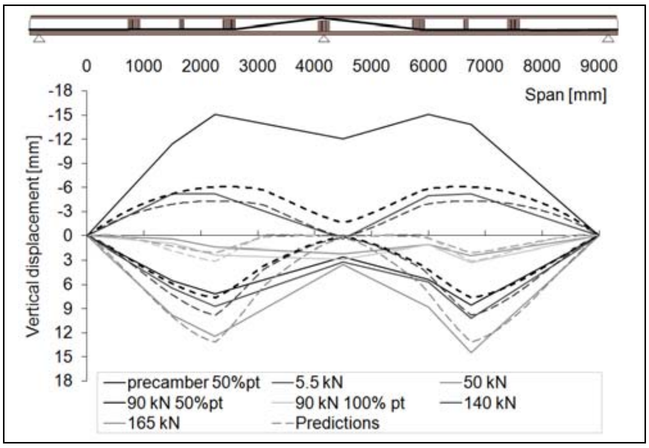

Figure27: *Beam 2 - Comparison of numerical and experimental displacement: Straight profile centrally draped*

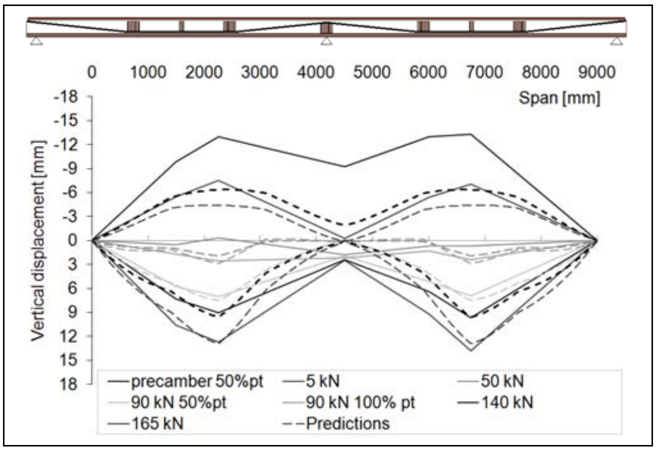

Figure 28: *Beam 2 - Comparison of numerical and experimental displacements: Draped profile*

Beams at this stage are working as simply supported, since the third support is not activated. It can be clearly seen in the graphs above that the beams are lifting up when pre-stressed. For such beams (in half-scale) their slenderness becomes relevant and small differences in pre-stressing force can produce high deformations.

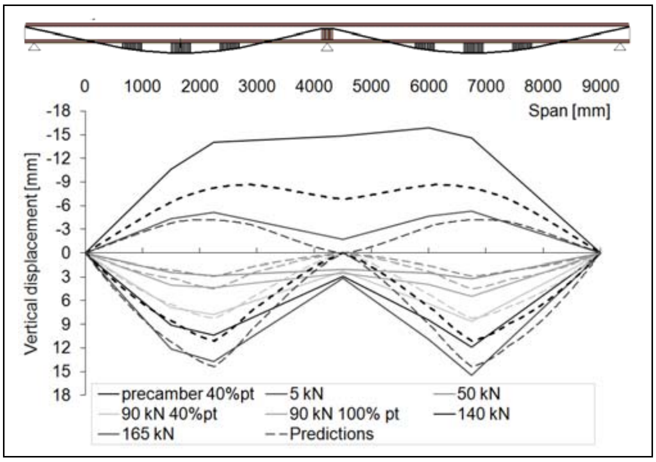

Figure 29: *Beam 2 - Comparison of numerical and experimental displacement: External profile*

Table 6: *Beam 2: Maximum deflections experimental (white column) and numerical (grey column)*

	Displacement							
Load [kN]	Benchmark		Bottom		Top		External	
0 (half pt)	0,00	0,00	-12,46	-6,06	-11,49	-6,34	-15,28	-8,25
5 (half pt)	1,10	-	-5,22	-4,78	-6,11	-4,40	-5,22	-4,21
50 (half pt)	7,85	7,22	1,99	2,04	0,15	1,92	3,02	2,90
90 (half pt)	13,95	12,86	7,84	7,63	7,01	7,50	8,20	8,23
90 (full pt)	13,95	12,86	2,85	3,18	2,82	2,80	4,90	4,40
110 (full pt)	16,98	15,68	6,03	-	5,02	-	7,12	-
140 (full pt)	-	-	9,44	9,79	9,19	9,57	11,15	11,10
165 (full pt)	-	-	13,29	13,13	13,12	12,91	14,53	14,38

Note: pt stands for post-tensioning

Table 6 confirm the enhanced performance of post-tensioned timber beams with respect to traditional solutions; post-tensioning is more effective for this scheme with a reduction of displacements up to 70%.

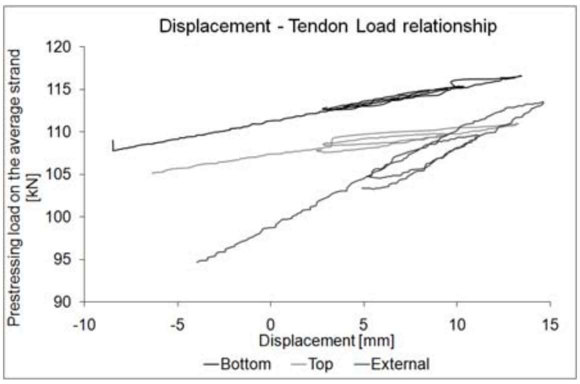

Figure 30: *Beam 2 – Displacement / tendon load relationship*

The same good correspondence between Bottom and Top configurations found for the simply supported beam can be observed; the same general considerations already discussed are thus valid for this specimen as well.
Figure 30 shows the increase of tendon force which can be quantified in a percentage of 5-10% for almost all cases.

5.3 CONSIDERATIONS

5.3.1 Statically determinate beam

In terms of elastic modulus the different beams are equivalent except for the configuration of external tendons where the equivalent elastic modulus results were amplified by 11-15% in comparison with the benchmark. The load variation respect to displacement shows a clear linear dependency as expected between displacement and tendon forces. High eccentricity of the external solution provides higher elongation than internal tendons and, for this reason, also a higher increment of tension force in the tendons.

As discussed previously, Force-Displacement graphs show how the three solutions can be considered similar to each other in the general behaviour (Figure 31).

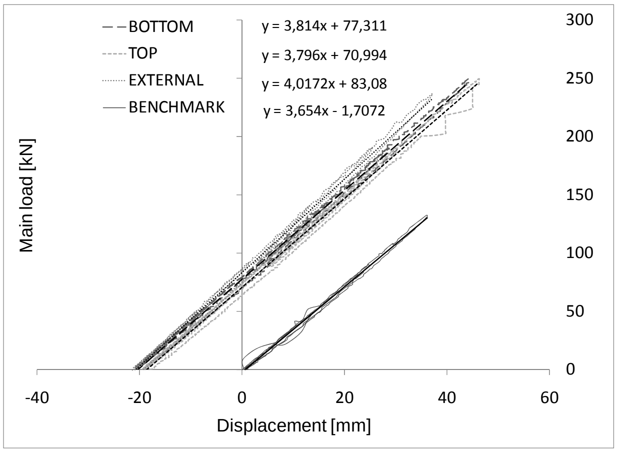

Figure 31: *Middle span displacement for each technology (simply supported beams) and trend lines*

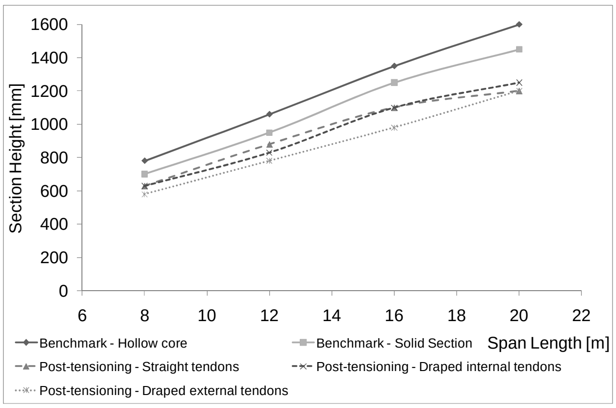

Figure 32: *Span length / Section height relationship for simply supported beam with a concrete slab floor*

After the precamber phase it can be noticed the increase of stiffness of the draped external solution due to the greater elongation of the strands and the relative increase of resistance.
It is important to notice how the introduction of post-tensioning technologies can double the capacity of the member. Parametric studies on the simply supported beam have been carried out to demonstrate how post-tensioning can reduce the section depth in order to achieve reduction of construction costs and achieve architectural benefits. Data show similarities between the three different configurations and the advantages with respect to benchmark solutions (Figure 32). The possible maximum saving of material obtainable with the post-tension solutions can reach up to 50% over a traditional LVL solid section (Figure 32).

5.3.2 Statically indeterminate beam

The similarity between draped internal and straight configurations can be highlighted within Force-Displacement graphs, where the general behaviour is shown in relation to the benchmark (Figure 33). As previously mentioned the increment of stiffness due to bigger elongation of the strands can be observed from the trend lines graph.

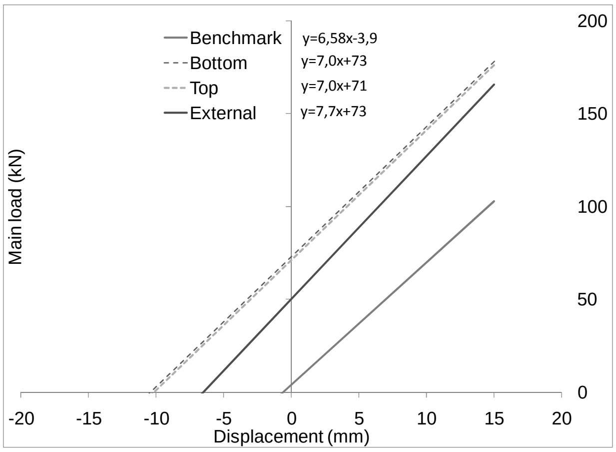

Figure 33: *Middle span displacement trend lines for each technology (indeterminate beams)*

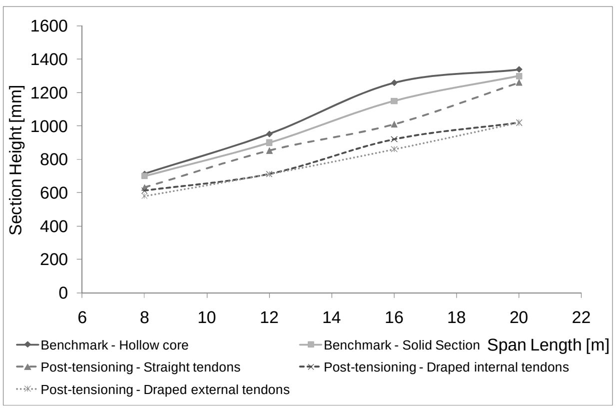

Figure 34: *Span length / Section height relationship for statically indeterminate beam with a concrete slab floor*

Results from parametrical analysis confirm a more significant efficiency of the draped solutions respect to the straight ones (Figure 34). However the overall

advantage of the technology is remarkable for either medium or long span beams in terms of section height.
Increased benefits have been found with a reduction of LVL material. Statically indeterminate post-tensioned beams can achieve 70% timber reduction especially if long span solutions are considered.

6 CONCLUSIONS

Numerical and experimental investigations confirm the enhanced performance of longitudinally post-tensioned timber beams. Post-tensioned tendons can induce a precamber in the beam and apparently reduce the resulting load scenario.
The non-linear increment of stiffness of the beam due to the presence of tendons can be considered negligible for internal configurations. So far, the design based on equivalent static forces can still be adopted, although it is not valid for external tendons running out of the section. Non-linear iterative procedures and reduced initial pre-stressing force are suggested for such cases since an increase of stiffness of around 10-15% in the beams due to the elongation of the strands has been recorded during testing.
While eccentricity at beam edges and deviation angle are key parameters for design, straight low and curved shaped internal tendon profiles for simply supported beams gave very similar results.
For continuous beams over several supports, the straight low tendon profile is not structurally the most viable solution. A highly eccentric tendon profile is better because it can drastically reduce the pre-stressing reinforcement, i.e. the number of tendons and anchors.
Despite the cost of pre-stressing technology, a great reduction of materials and weight compensate within the total cost of the structure which remains competitive with traditional timber beams.

ACKNOWLEDGEMENT

The present research project has been funded by the Structural Timber Innovation Company (STIC). LVL was supplied by Nelson Pine, strands provided by BBR – ConTech, and the manufacturing by Hunter Laminates The technical support of John Maley is also gratefully acknowledged.

REFERENCES

[1] Giorgini S.: Service load analysis and design of long span unbonded post-tensioned timber beams, Technical University of Milan, MSc thesis, 2009.
[2] Davies M.: Long Term Behaviour of Laminated Veneer Lumber (LVL) Members Prestressed with Unbonded Tendons, University of Canterbury, New Zealand, 2007.
[3] http://www.nzwood.co.nz/why-wood/timber-design-awards-2009
[4] Taylor R. J. and Csagoly P. F. Transverse Post-Tensioning of Longitudinally Laminated Timber Bridge Decks. Transportation Research Board, TRR 665 Vol. 2 Washington DC, 1978.
[5] Csagoly P. F. And Taylor R. J. A Structural Wood System for Highway Bridges. International Association for Bridge and Structural Engineering. IABSE, Periodical 4/1980, P-35/80, pp 157-183. Vienna (also MTO Report SRR-80-05), 1980 b.
[6] Taylor, R. J. et al. Prestressed Wood Bridges. Ministry of Transportation Ontario SRR-83-01, 1983.
[7] Crews, K. I. Behaviour and Critical Limit States of Transversely Laminated Timber Cellular Bridge Decks, PhD Thesis, 2002.
[8] Priestley, M. J. N. Overview of the PRESSS Research Program, *PCI Journal*, 36(4): 50-57, 1991.
[9] Priestley, M. J. N. The PRESSS Program–Current Status and Proposed Plans for Phase III, *PCI Journal*, 41(2): 22-40, 1996.
[10] Priestley M. J. N., Sritharan S., Conley J. R. and Pampanin S. Preliminary Results and Conclusions from the PRESSS Five-story Precast Concrete Test-building, *PCI Journal*, 44(6): 42-67, 1999.
[11] Pampanin, S. Emerging Solutions for High Seismic Performance of Precast/Prestressed Concrete Buildings, *Jo. of Adv. Concrete Technology*, invited paper "High performance systems", 3(2): 202-223, 2005.
[12] Palermo A., Pampanin S., Buchanan A., and Newcombe M. Seismic Design of Multi-storey Buildings using Laminated Veneer Lumber (LVL). In: NZSEE Annual Conference, CD-ROM, 2005.
[13] Palermo A., Pampanin, S., Fragiacomo, M., Buchanan, A. H. and Deam B. L. Innovative Seismic Solutions for Multi-storey LVL Timber Buildings. In: 9th World Conference on Timber Engineering, CD-ROM, 2006.
[14] Smith T., Ludwig F., Pampanin S., Fragiacomo M., Buchanan A., Deam B., and Palermo A. Seismic Response of Hybrid-LVL Coupled Walls under Quasi-static and Pseudo-dynamic Testing. In: NZSEE Annual Conference, CD-ROM, 2007.
[15] Pres-Lam® system, Prestressed Timber Ltd, 2009.
[16] Smith T., Ludwig F., Pampanin S., Buchanan A., Fragiacomo M. Feasibility and Detailing of Post-tensioned Timber Buildings for Seismic Areas. In: NZSEE Annual Conference, 2008.
[17] Balanguru, P. N. Increase of stress in unbonded tendons in prestressed concrete beams and slabs, *Canadian Journal of Civil Engineering*, 36: 262-268, 1981.
[18] Naaman A. Partial Prestressing in the Rehabilitation of Concrete Bridges. In: U.S.-European Workshop on Bridge Evaluation, Repair and Rehabilitation, St. Rèmy-lès-Chevreuse, 391-406, 1987.
[19] Naaman A. New Methodology for the Analysis of Beams Prestressed with External or Unbonded Tendons, External Prestressing in Bridges, SP-120, American Concrete Institute, Detroit, 339-354, 1990.
[20] Naaman A. E. and Alkhairi F.M. Stress at Ultimate in Unbonded Post-Tensioning Tendons: Part 1 – Evaluation of the State-of-the-Art, *ACI Structural Journal*, 88: 683-692, 1991.
[21] Timoshenko S.: Strength of materials, D. Van Nostrand Company, Inc., 1930